ELSEVIER

Physica B 221 (1996) 469–486

PHYSICA B

Electron-density maps for the Si(1 1 1) 7 × 7 surface calculated with the maximum-entropy technique using X-ray and electron-diffraction data

C.A.M. Carvalho[b,1], H. Hashizume[a,*], A.W. Stevenson[c], I.K. Robinson[d]

[a] *Research Laboratory of Engineering Materials, Tokyo Institute of Technology, 4259 Nagatsuta, Midori-Ku, Yokohama 226, Japan*
[b] *Inst. de Física, Univ. de São Paulo, Brazil*
[c] *CSIRO Division of Materials Science and Technology, Clayton, Australia*
[d] *Department of Physics, University of Illinois, Urbana, IL 61801, USA*

Abstract

Maximum-entropy electron-density maps have been calculated for the first time for a two-dimensional surface structure using X-ray and electron-diffraction data. The maps clearly resolve all the 102 atoms of the Takayanagi dimer-adatom-stacking-fault model. The atomic positions determined from the map are in good agreement with those from a least-squares refinement. Electron bondings between atoms are not apparent in the maps due to insufficient data quality. The reliability of the maximum-entropy method is discussed. It is shown that the calculation procedure must be continued to values of $\chi^2 < 1$ in most cases. A method to estimate the uncertainty in the density values and to identify reliable features in the maps is presented. It is shown that the maximum-entropy method is a promising technique to obtain detailed structure information from a small number of accurate structure factors.

1. Introduction

The level of characterization of materials required by present-day technology has reached a point where detailed knowledge of the atomic structure of surfaces is important. The surface has a different environment from the bulk, resulting in reconstruction and relaxation of atomic structures in near-surface layers of crystals. Accurate surface-electron densities are required for a better understanding of the origin and nature of the reconstruction, as well as chemical bonding and electronic properties of the surface.

Grazing-incidence X-ray diffraction is a powerful technique to determine surface structures [1]. X-ray scattering from surfaces is well described by the simple kinematical theory, allowing direct access to the moduli of the Fourier coefficients of the electron-density distribution. Samples often need to be placed in an ultrahigh vacuum environment to avoid contamination and denaturalization of the structure under investigation. The geometry of grazing-angle diffraction, combined with the design of a practical vacuum chamber, limits the accessible reciprocal space. The small X-ray scattering power and geometric effects make high-angle reflections hard to measure, further reducing the number of measurable Bragg reflections, with the consequence being a low resolution and distortions in electron-density maps calculated with the Fourier synthesis method. Due to the small glancing-incidence angles, a large sample area is

*Corresponding author.
[1] Present address: Dpto. de Física, Univ. Federal do Paraná, Curitiba, Brazil.

SSDI 0921-4526(95)00968-X

illuminated, but in many cases the structure is well ordered only in a small area. This introduces errors in the structure-factor data, which can be evidenced by the significantly different intensities of equivalent reflections.

The transmission electron-diffraction technique allows a greater number of surface Bragg reflections to be observed from a smaller sample area. Dynamical effects arising from the bulk substrate are significant, however, notably in low-angle regions, which seriously influence the surface reflections. This complicates the interpretation of the data. In many aspects, electron diffraction is complementary to surface X-ray diffraction.

The electron density divided by the number of electrons in the unit cell is the probability of finding electrons in a given position. The maximum-entropy (ME) method is a technique to infer a probability distribution from the available information. It uses *only* the available information and the inferred distribution is totally unbiased, in the sense that no arbitrary hypothesis is made in the calculation process. In particular, it does not assume zero amplitudes for unmeasured reflections, which reduces the truncation effects encountered in the Fourier synthesis method. The distribution is obtained by maximizing the entropy under constraints built from the data [2]. This characteristic of the ME method can be exploited in the determination of accurate electron-density maps for surface structures. The present paper describes an attempt to calculate such maps for the Si(1 1 1) 7×7 surface using X-ray and electron-diffraction data. Discussion will also be extended in order to address doubts about the ME method raised recently.

2. The Si(1 1 1) 7×7 structure

The Si(1 1 1) 7×7 surface reconstruction is the most complex one ever discovered, which makes it a good test case for the ME method. Fig. 1 shows the widely accepted model structure of Takayanagi et al. [3], projected on the (1 1 1) plane. In this model, reconstruction takes place on the three top layers of atoms; the underlying layers are almost undisturbed and the atoms are at the bulk positions slightly displaced along the surface normal. The 7×7 units cell is rhombohedral, with lattice vectors $\boldsymbol{a} = \frac{7}{2}[1\,0\,\bar{1}]$ and $\boldsymbol{b} = \frac{7}{2}[\bar{1}\,1\,0]$ in the usual cubic system. These vectors are seven times longer than the ones defining the unreconstructed 1×1 surface. The top layer contains 12 atoms in the cell (large open circles), located at A sites if we designate the fourth layer as an A layer of the face-centered cubic lattice, and is called the *adatom* layer. The second one, the *stacking-fault* layer, contains 42 atoms (small open circles). The 21 atoms in the right triangular subcell are located at B sites of the bulk silicon, but the 21 atoms in the left subcell are at C sites. The *dimer* layer, the third one, has 15 atoms at A sites in each subcell plus 9 pairs of dimers on the edges of the triangular subcells (filled circles). Atoms in the underlying unreconstructed layers occupy A sites in the first layer, and C sites in the next layer. These layers are shown by a hexagonal network in Fig. 1. This structure, known as the dimeradatom-stacking-fault (DAS) structure, has 102 reconstructed atoms in the cell, and contains a patch of stacking faults in the left subcell where layers are stacked in the order of $CAAC + A$adatoms. All the 12 adatoms in the DAS model have third-layer atoms immediately below.

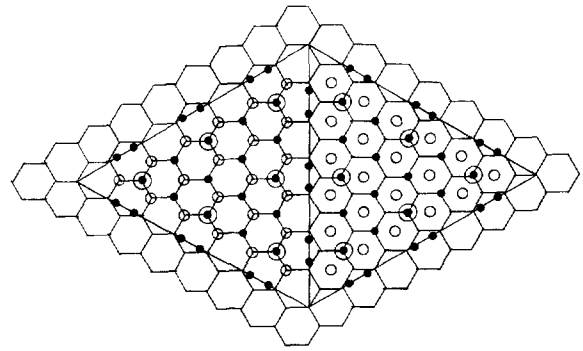

Fig. 1. Top view of the dimer-adatom-stacking-fault model for the Si(1 1 1) 7×7 structure. Large open circle: top-layer adatoms; small open circle: second-layer stacking-fault atoms; filled small circle: third-layer dimer atoms. The hexagonal network shows the silicon atoms in the fourth and fifth unreconstructed layers.

The structure has the symmetry of the plane group p6mm. The minimum asymmetric unit (MAU) of this group is a triangle with vertices at (0, 0), $(\frac{1}{2}, 0)$ and $(\frac{2}{3}, \frac{1}{3})$. There are mirror planes on each side of the MAU, a 6-fold axis at the origin, a 2-fold axis at $(\frac{1}{2}, 0)$ and a 3-fold axis at $(\frac{2}{3}, \frac{1}{3})$. The presence of a mirror along the short diagonal of the 7×7 cell is consistent with the stacking fault in one subcell, because the diamond structure of bulk silicon has no such symmetry.

The X-ray data for our ME calculation consist of the structure-factor moduli of 84 in-plane reflections ($l = 0$), collected by Robinson et al. [4] with 1.3 Å X-rays. The set only includes fractional-order reflections with non-integer h and/or k indices, and has a resolution $1/H_{\max} = 1.135$ Å, where $H_{\max}$ is the length of the longest scattering vector measured. There are "holes" in the sampling of the reciprocal space. These data are a subset of about 120 reflections which were used by Robinson et al. [4] to refine the DAS model with a standard crystallographic least-squares (LSQ) method. Their refinement assumed the p6mm symmetry. The reconstructed atoms are found to be slightly displaced from the ideal DAS positions; the structure is strained. We determined the

phases (0 or π) of the 84 structure factors using the refined atomic coordinates; the phases are the same as those obtained from the ideal DAS model, except for one reflection. Values for Si atomic scattering factors were taken from the International Tables for Crystallography [5], to which interpolated anomalous dispersion corrections $f' = 0.203$ and $f'' = 0.255$ were applied.

Our transmission electron diffraction (ED) data consist of the structure-factor moduli of 193 fractional-order reflections with $l = 0$, measured by Twesten and Gibson [6]. The resolution is 0.873 Å, which is similar to that of the X-ray data, but there are almost no "holes" in the reciprocal-space sampling. Only 16 reflections have indices higher than the highest X-ray reflection. In order to minimize the effects of the dynamical bulk diffraction, the sample was tilted by a few degrees from the zone axis. In addition, the measured intensities of the surface reflections were averaged over equivalent reflections, which appeared in different reciprocal-space areas and were affected by the bulk diffractions to different extents.

An LSQ refinement of the DAS model using this data by Twesten and Gibson [6] found atomic positions very similar to those of Robinson et al. [4], but not identical. This suggests that the ED structure factors were essentially correctly measured, even though they may not be completely free from dynamical contaminations. We determined the structure-factor phases from the atomic positions given by the LSQ refinement. Some of the coordinates indicated by Twesten and Gibson [6] are misprinted; the y coordinate for atoms 5 and 7 should be 0.3864(4) and 0.3824(4), respectively. The phases thus obtained are different from those calculated from the DAS positions for 25 reflections. If we use the positions obtained in the X-ray refinement, 12 reflections have opposite signs, of which only three are present in our X-ray data set. The atomic scattering factors were calculated from the X-ray ones with Mott's formula.

The errors in both sets of data come from measurement uncertainties and also from the intensity spreads of equivalent reflections.

3. Principle of the maximum-entropy method

The electron-density distribution $\{\rho_i\}$ is determined at N points in the unit cell by maximizing the entropy under constraints, which describe the available information on the distribution. The expression of the entropy S, due to Shannon and Jaynes, is given by

$$S = -\sum_{i\in \mathrm{uc}} \rho_i' \ln \frac{\rho_i'}{\tau_i'}, \tag{1}$$

where uc means the unit cell, $\rho_i' = \rho_i / \sum_j \rho_j$, $\tau_i' = \tau_i / \sum_j \tau_j$ and $\{\tau_i\}$ is a prior distribution.

The entropy is maximized under two constraints. The first is that the integral of the density equals the number Z of electrons in the unit cell, that is, $\sum_i \rho_i = Z$. The second constraint is $\chi^2 = C$, where C is a constant that is discussed below and

$$\chi^2 = \frac{1}{R}\sum_{\boldsymbol{h}} \frac{1}{\sigma_{\boldsymbol{h}}^2} |F_c(\boldsymbol{h}) - F_{ob}(\boldsymbol{h})|^2.$$

F_{ob} are the observed structure-factor amplitudes and F_c are those calculated from the distribution $\{\rho_i\}$. $\sigma_{\boldsymbol{h}}$ is the standard deviation of $|F_{ob}(\boldsymbol{h})|$ and R is the number of reflections. The density in this context is a real quantity representing the number of electrons in a volume element. Since the structure is centrosymmetric, we used the modulus of the structure factor (not the real part) with the sign given by the refined model.

To perform a constrained maximization of S (Eq. (1)) the technique of Lagrange multipliers is used. We seek the unconstrained maximum of

$$Q = S - \frac{\lambda_1}{2}\chi^2 - \lambda_3\left(\frac{A}{N}\sum_j \rho_j - Z\right),$$

where the λ's are constants to be determined and A is the area of the unit cell. The last term on the right-hand side represents the normalization of the density. The maximum of Q is obtained by setting $\partial Q/\partial \rho_k = 0$. Following the derivation described by Carvalho and Hashizume [7], we get

$$\rho_k = \tau_k \exp\left\{\Lambda \sum_{\boldsymbol{h}} \frac{1}{\sigma_{\boldsymbol{h}}^2} \mathscr{R}\left[[F_{ob}(\boldsymbol{h}) - F_c(\boldsymbol{h})] \sum_l e^{-i2\pi \boldsymbol{h}\cdot \mathbf{O}_l \mathbf{r}_k}\right]\right\}, \tag{2}$$

where Λ is a multiple of λ_1, $\mathscr{R}$ is the real part of a complex quantity and the sum over l runs through the symmetry operations of the space group. The density is calculated only in the MAU. The structure factors are given by

$$F_c(\boldsymbol{h}) = \frac{A}{N}\sum_{k\in \mathrm{mau}} \frac{\rho_k}{p_k} \sum_l e^{+i2\pi \boldsymbol{h}\cdot \mathbf{O}_l \mathbf{r}_k}, \tag{3}$$

where p_k is the number of times a position is reproduced when all the symmetry operations are applied to it.

Eq. (2) for the density is transcendental and must be solved by successive iterations. We start from the uniform distribution $\rho_k = F_0/N$, calculate the structure factors $F_c(\boldsymbol{h})$ from Eq. (3), substitute them in the right-hand side of Eq. (2) and obtain a new distribution. We repeat the procedure until $\chi^2 = C$ is reached. The initial uniform distribution is obtained if the entropy is maximized under no constraint, that is, without any available information. Therefore, the assumed initial distribution introduces no bias in the calculation. We used the algorithm that

was successfully applied to the determination of electron densities in $Mg_3BN_3(L)$ crystal from X-ray powder diffraction data [8, 9]. The value of Λ only influences the rate of convergence, not the final map; if it is too large the iteration does not converge. Generally speaking, the maximum permissible value of Λ is smaller for data with smaller errors. This is easily seen from the form of Eq. (2).

Now let us discuss the constraint $\chi^2 = C$. The first choice is to use $C = 1$. In standard fitting procedures a value of χ^2 greater than 1 implies a poor agreement of the calculated distribution with the data. A value less than 1 means overfitting where artifacts are produced in the corresponding maps. $\chi^2 = 1$ means that the calculation is in statistical agreement with the data and that all information in them has been explained by the calculation. However, it has been pointed out [10, 11] that the distribution of the residues $[F_c(\boldsymbol{h}) - F_{ob}(\boldsymbol{h})]^2/\sigma_h^2$ does not follow a Gaussian distribution as expected. Instead, the ME method often (but not always) tends to strongly concentrate the residues on a few reflections, usually among the strongest ones, while the other residues come up much smaller than 1. One might think that these few reflections are in error for some reason. If, however, they are removed from the data set and the maximization performed again, other reflections, which were almost exactly reproduced before, will now concentrate the residues, clearly showing that the problem is not in the data.

The reason is that the ME method is *not* a process to fit model parameters to the data. It is a method to calculate a probability distribution without using *any* model. This is evident from the number of "degrees of freedom" in the "fit": the density is calculated at many more points than the number of reflections. The statistical meaning of χ^2 is thus not applicable to the entropy maximization; it can only be used as a measure of how far from the data is the Fourier transform of the calculated distribution. Since the deviations are usually large for certain reflections when $\chi^2 = 1$, the density obtained under this constraint is in fact calculated for a set of Fourier coefficients that are different from the data. To obtain a distribution whose Fourier coefficients agree with the structure factors, the iteration process must be continued until no significant changes occur in the distribution features. The final value of χ^2 to be reached depends on the data and their errors. It may happen that the distribution is not sensitive to the value of a given reflection and a large residue is irrelevant. Also, for precise enough measurements, $\chi^2 = 1$ implies that the Fourier coefficients of the distribution are already so close to the measured structure factors that going closer to them does not produce significant changes. This is the reason for the good results obtained in many ME calculations using precisely measured structure-factor data and stopped at $\chi^2 = 1$.

One could argue why to use the χ^2 as a constraint instead of R constraints of the form $F_c(\boldsymbol{h}) = F_{ob}(\boldsymbol{h})$ (so-called hard constraints), since we cannot rely on its statistical significance. In the limit of $\chi^2 = 0$ both methods produce the same result. There is a practical reason for using the χ^2 constraint (so-called soft constraint). We must solve Eq. (2) while the R constraints lead to a system of R exponential equations for the Lagrange multipliers, which is difficult to solve. Also, in our case, the software for the χ^2 constraint is readily available.

We now consider the influence of the data uncertainties on the calculated distribution. If one goes to sufficiently low χ^2, they do not affect the distribution, which is determined, as mentioned above, only by the $F_{ob}(\boldsymbol{h})$. However, if the experiment were repeated a number of times, the structure factors would fluctuate around their mean values. It is necessary to know the influence of these fluctuations on the calculated electron density. Only those features common to most of the resultant distributions are reliable; other features are ascribed to data noise. Since we cannot repeat the experiment several times, we use the following computer-simulation approach: we generate "fluctuated data sets" $F_{ob}^{(j)}(\boldsymbol{h}) = F_{ob}(\boldsymbol{h}) + \sigma(\boldsymbol{h})\delta^{(j)}$, where $\delta^{(j)}$ is a random variable with a normal distribution of mean 0 and variance 1.

The ED structure factors are the Fourier coefficients of the electric potential in the crystal. One could try to use ME to calculate it, but the potential is not a probability distribution. Even if we try to do this anyway, it is necessary to ensure that the potential is always positive everywhere, even for non-spherical atoms, but this is not obvious. Another difficulty is that the solid foundation for the ME method as the one method to calculate a distribution from available information without any implicit hypothesis does not apply to functions that are not probability distributions. Therefore, we can only justify it on the pragmatical grounds of the good/bad results it produces.

Here we take another approach to extract the electron-density information from the ED data. For a general crystal, Mott's formula applied to the unit cell gives

$$F(\boldsymbol{h}) = 0.023934\left(\sum_i Z_i e^{i2\pi \boldsymbol{h}\cdot\boldsymbol{r}_i} - \boldsymbol{h}^2 V(\boldsymbol{h})\right),$$

where V is the Fourier transform of the potential and Z_i is the atomic number of the constituent atoms. One undesirable aspect of this formula is that it is necessary to know the positions of the atoms to evaluate $F(\boldsymbol{h})$. One may use the positions that determine their phases, but this means that the model positions affect the structure-factor amplitudes themselves, not only their signs, which has a much stronger influence. In our particular case it is possible to avoid this. We recall that since silicon has

only one type of atom, $V(\boldsymbol{h}) = f_{el}(\boldsymbol{h})E$ and $F(\boldsymbol{h}) = f_{xr}(\boldsymbol{h})E$, where E is a sum of exponentials. Thus

$$F(\boldsymbol{h}) = V(\boldsymbol{h}) f_{xr}(\boldsymbol{h}) / f_{el}(\boldsymbol{h}). \quad (4)$$

All ME maps presented below for the ED data were calculated using the structure factors obtained by the above relation. The uncertainties are also multiplied by the factor f_{xr}/f_{el}.

4. Electron-density maps for the Si(1 1 1) 7 × 7 surface

The number of points on the ***a*** and ***b*** axes was chosen to be a multiple of 3 and 7, so that there is a grid point at the center of all atoms in the ideal DAS structure. The number of points on the two axes must be the same, otherwise a symmetry operation applied to a grid point may not result in another grid point. Most of the calculations were done with a sampling on each axis about four times denser than half of the data resolution ($1/2H_{max}$); we recall that $1/2H_{max}$ is the minimum sampling necessary to prevent errors in the Fourier transformations. The remaining calculations were done with a grid eight times denser. It is important to use a sampling step smaller than the Fourier resolution because, unlike the distribution obtained by Fourier synthesis, the ME distribution is not band-limited.

We will first discuss the general features of the X-ray maps. Then the discussion is extended to the ED maps and the characteristics of the ME method.

4.1. X-ray maps

Fig. 2 shows the ME map calculated from the X-ray data. All the 102 atoms in the DAS structure are clearly resolved. Since only fractional-order reflections are included in the calculation, the distributions in the faulted and unfaulted halves of the unit cell are identical. A few spurious peaks are seen but they are lower than the atomic peaks. Fig. 3 shows a magnified view around a minimum asymmetric unit. Spurious features are evident in the vicinity of atoms 3, 11 and 14, on the edge of the MAU, as well as between atoms 8 and 9. Some atoms, notably atom 8, have an elongated profile. The density is maximal at the position of atoms 2-13, were these two atoms overlap in the projection. The density is lower at position 1-11, which is another superposed-atom position, than at position 14 where only one atom is located.

A gray-scale plot of the ME density only shows 102 dots at the atom positions. To make visible low-density regions and high-density atoms with a reasonable contrast in a single plot, we filtered the density D through the function $D' = \log(1 + pD/D_{max})/\log(1 + p)$, where D_{max} is

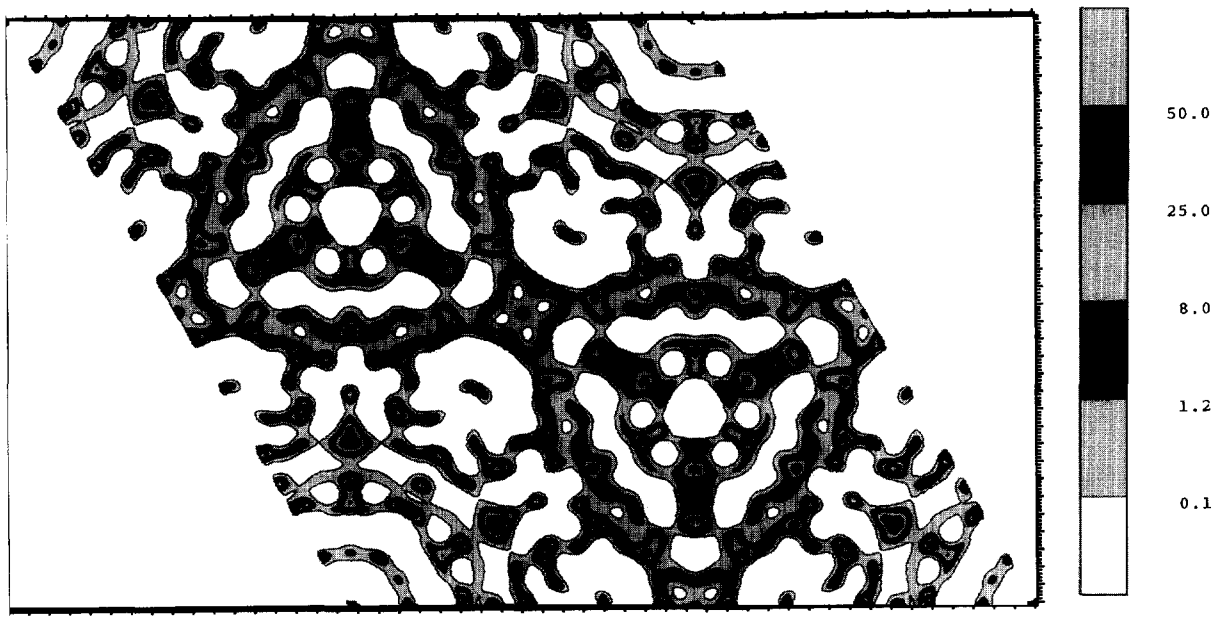

Fig. 2. Maximum-entropy electron-density map calculated for the Si(1 1 1) 7 × 7 surface from 84 in-plane X-ray reflections. 2 × 2 unit cells are shown. Contour lines are drawn for the densities shown on the right in units of e/Å^2.

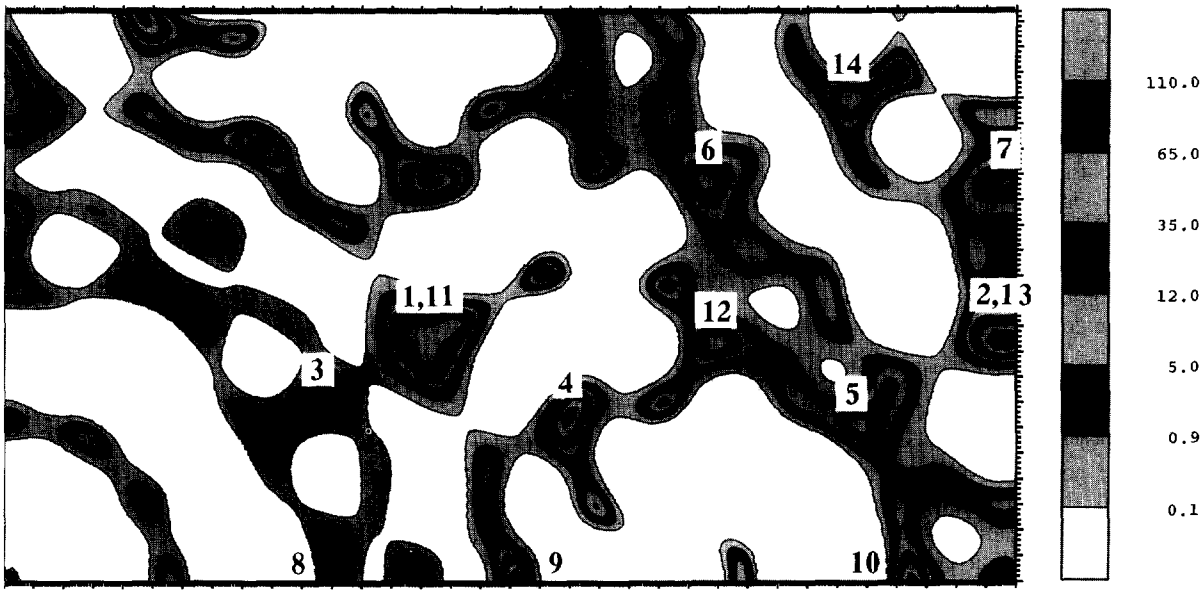

Fig. 3. Magnified view of Fig. 2. The minimum asymmetric unit of the 7×7 structure is shown with atoms numbered in the scheme of Ref. [4].

the maximum density. p is a parameter controlling the contrast of the image. If $p \ll 1$, D' is a linear function of D. If $p \gg 1$, D' is a logarithmic function of D. Fig. 4 shows plots with $p = 1 \times 10^4$ of X-ray and ED densities. These pictures give quite a different impression from scanning tunneling microscopy (STM) images, because STM can only reveal the 12 adatoms per unit cell while in the ME picture all the 102 atoms are visible. The black holes centered at the corners of the cell, i.e. corner holes [12, 13], are quite evident in the ME-picture. The topograph features dark stripes along the dimer rows and two very black small holes at the centers of the triangular subcells. The six adatoms adjacent to corner holes (atoms 1) appear weaker than the other six (atoms 2), because atom 1 has a lower density than atom 2 (see Fig. 3), in contrast with STM images of positively biased Si surfaces [12–14].

Fig. 5 shows a Fourier synthesis map of the same X-ray data. We see that densities are negative in large areas of the cell. Atoms 12 and 14 appear very weak, and there is a high artifact between atoms 9 and 10 that could be taken for an atom, since it is stronger than the peak of atom 14. The markedly low peaks at positions of atoms 12 and 14 are common features in Fourier maps calculated from data with missing integer reflections. These positions coincide with bulk positions in both the faulted and unfaulted subcells, and are not adatom sites. Hence, they are the most affected by the absence of the bulk-reflection data. The ME map displays high densities at these positions, evidencing that it is not seriously affected by the absence of integer reflections. This is because the ME method does not assume null intensities for missing reflections.

The ME map is significantly more sharply peaked and has a higher spatial resolution than the Fourier map. The longest scattering vector used in the calculations is (20, 1) in units of the 7×7 cell edges, which means a resolution of about 0.025 times the edge length. The high-density atomic peaks and structural details seen in Fig. 3 indicate that this resolution is largely exceeded in the ME map.

Taking advantage of this high spatial resolution, we tried to determine the positions of the atoms, assuming that their centers are located at the maxima in the electron-density map. The coordinates, as well as the contour plots, are calculated using bi-cubic interpolation by Preusser's algorithm FARB-E-2D [15].

Table 1 shows the coordinates determined from the ME map, together with the ones obtained by a standard least-squares fit by Robinson et al. and those from the ED map. Robinson et al. used about 120 reflections, which yield $\chi^2 = 1.6$, but only 84 of them were used in our ME calculation. The position of atom 8 is less precise because there are several maxima of the density with similar values at this position. This also happens to some other atoms, but the different maxima are very close to each other.

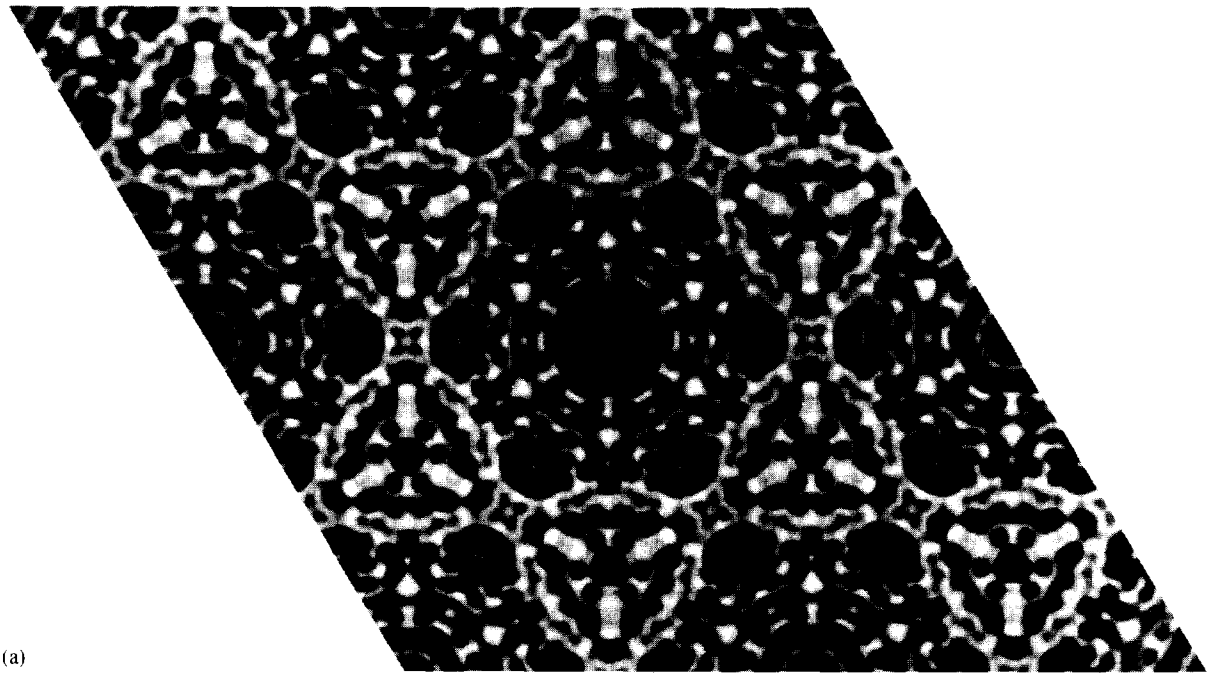

(a)

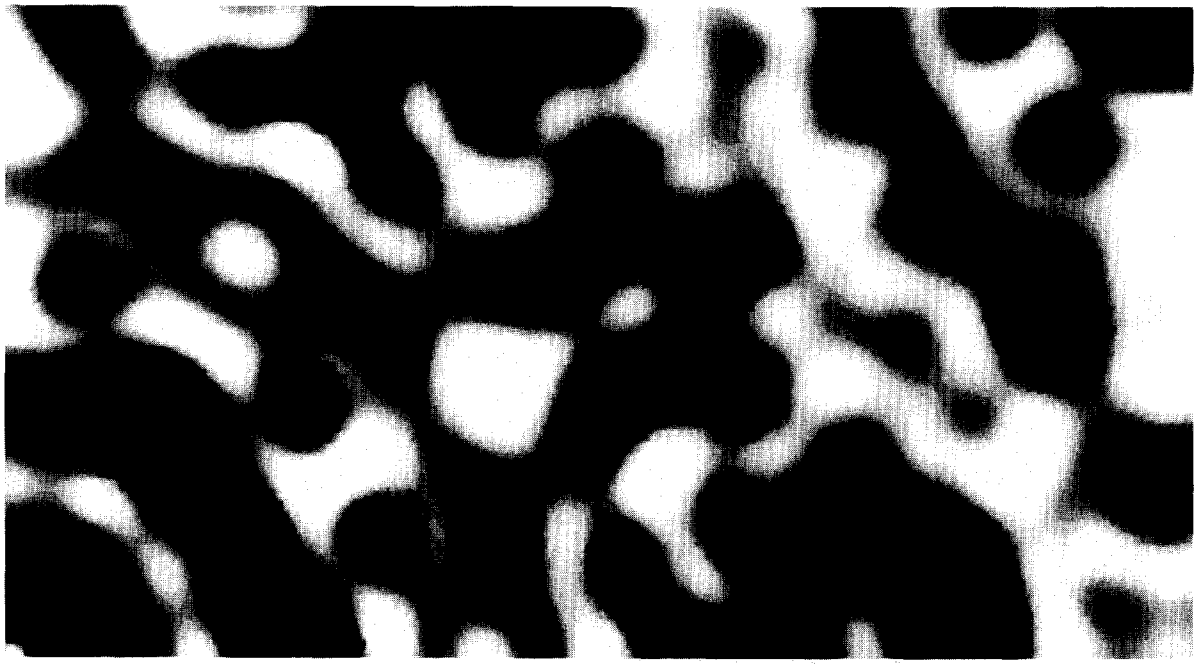

(b)

Fig. 4. Gray-scale plot of the electron densities calculated by the ME method. Regions of high density are white and regions of low density are black. The contrast parameter p (see text) is 1×10^{-4}. (a) X-ray map; (b) magnified view of (a); (c) magnified view of the ED map. Four Si(1 1 1) 7×7 cells are included in (a). The regions in (b) and (c) are the same as in Fig. 3.

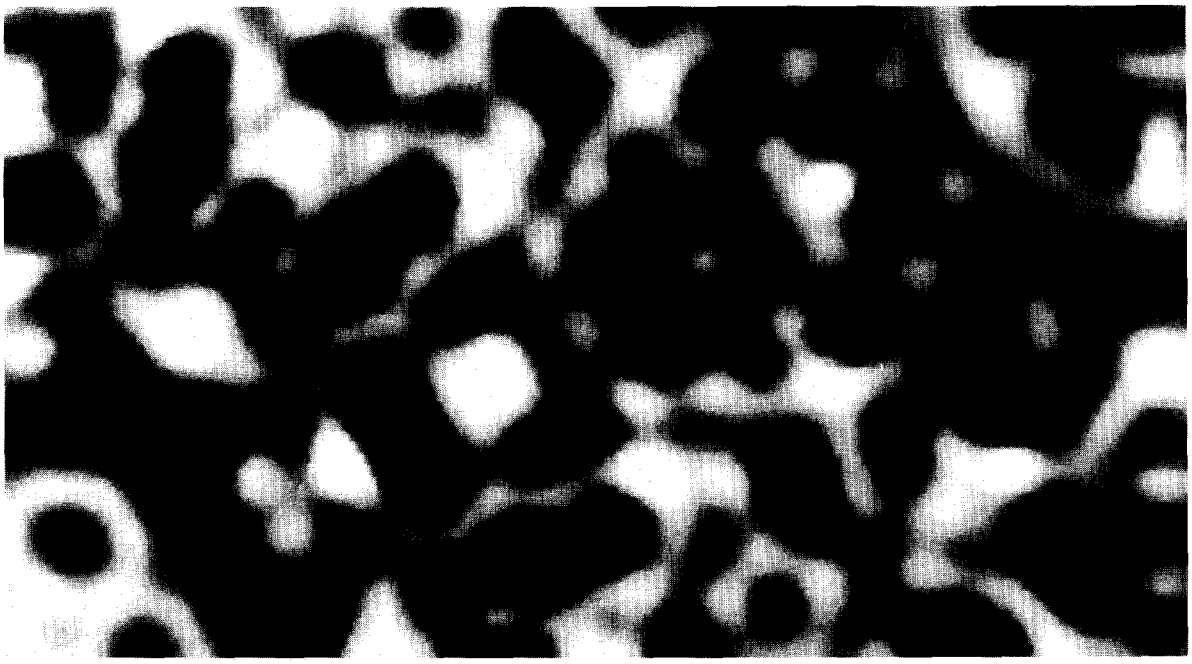

(c)

Fig. 4. (continued)

Fig. 5. Fourier synthesis map of the X-ray data. The region is the same as in Fig. 3.

Table 1
Atomic coordinates determined by maximum entropy and least squares

Atom	X-ray map		LSQ [Ref. [4]]		ED map		LSQ [Ref. [6]]	
	x	y	x	y	x	y	x	y
1	0.2984	0.1495	$2y$	0.1423	0.2889	0.1454	$2y$	0.1427
2	0.5709	0.1409	$(y+1)/2$	0.1420	0.5727	0.1444	$(y+1)/2$	0.1440
3	0.2090	0.1044	$2y$	0.0978	0.1990	0.1002	$2y$	0.0987
4	0.3308	0.0961	0.3298	0.0959	0.3278	0.0947	0.3258	0.2305
5	0.4744	0.0909	0.4802	0.0947	0.4825	0.0950	0.4819	0.0955
6	0.4695	0.2351	$2y$	0.2368	0.4770	0.2389	$2y$	0.2370
7	0.6173	0.2335	$(y+1)/2$	0.2326	0.6176	0.2338	$(y+1)/2$	0.2352
8	0.1669	0.0032	0.1664	0	0.1609	0.0006	0.1656	0
9	0.2564	−0.0002	0.2579	0	0.2590	0.0004	0.2584	0
10	0.4553	0.0017	0.4540	0	0.4561	0.0011	0.4545	0
12	0.4264	0.1398	$2y$	0.1404	0.4261	0.1393	$2y$	0.1395
14	0.5661	0.2832	$2y$	0.2851	0.5697	0.2850	$2y$	0.2840

It is to be noted that the ME positions nearly satisfy the relations imposed by the p6mm symmetry. This means that the symmetry hypothesized in the least-squares refinement actually exists in the structure.

We observe in Figs. 2 and 3 complicated low-density ridges, which do not protrude towards the adjacent atoms, both in the surface and the bulk, to which they are bonded in the DAS model. How reliable are these features? Fig. 6 shows two maps produced by randomly fluctuating the X-ray data. One can see that there are large variations, both in the low- and high-level contours. In an attempt to identify the reliable features, we computed seven fluctuated maps and calculated, at each point, the standard deviations of the densities. We show in Figs. 7 and 8 the original density (Fig. 3) minus the deviation, a lower map, and plus the deviation, an upper map. We remark that no real map can be like the upper and lower maps shown here, because these are not normalized to the number of electrons in the unit cell. Any real map will lie between the upper and lower ones, being closer to one or the other in different regions, as can be seen by Fig. 6. Furthermore, the distribution of density values among the fluctuations, for a fixed point in the cell, is not Gaussian, due to the highly non-linear nature of the ME method. The distribution varies from point to point and is asymmetric, especially for the lower values of the density. A large part of the cell in the lower map is negative, showing that the standard deviation overestimates the spread of density values on the lower side. We displayed the negative values in the same way as the small positive ones in the picture. This way the pictures show an estimation of the density spread. Common features in these two pictures can be trusted, differences cannot. Fig. 7 shows almost no low-level contours, indicating that nearly all spurious peaks, except those on the dimer rows, can be attributed to data noise. It also shows that very little information about bondings are reliable, such as a few low contours between atoms 2-13 and 7, and between atoms 5 and 10. Furthermore, there are significant differences in the densities at the atomic positions, meaning that the peak values cannot be trusted. This explains the strange peak-height relations described above. It can also be observed that some spurious peaks and the elongated profile of atom 8 are present in all the maps, so they cannot be attributed to data fluctuation. This is not a problem of the ME reconstruction, because the Fourier synthesis (Fig. 5) manifests the same phenomenon, to a lesser extent. One might think that the number of reflections is too small to adequately recover the shapes of all atoms. We will show, however, that this is not the case.

Fig. 9 shows an ME map calculated using the theoretical structure factors obtained from the LSQ refined positions, for the same 84 reflections. It is seen that all atoms, except atom 9, are spherical in the higher-level contours, and that there are no spurious peaks. This high-quality picture shows that the artifacts in the map obtained from the experimental data, and not explained by the fluctuations, are a consequence of the inaccuracy of the data, possibly beyond the uncertainty of some reflections.

4.2. Maps from ED data

Let us now look at maps calculated from the ED data to see the influence of the number of reflections on the

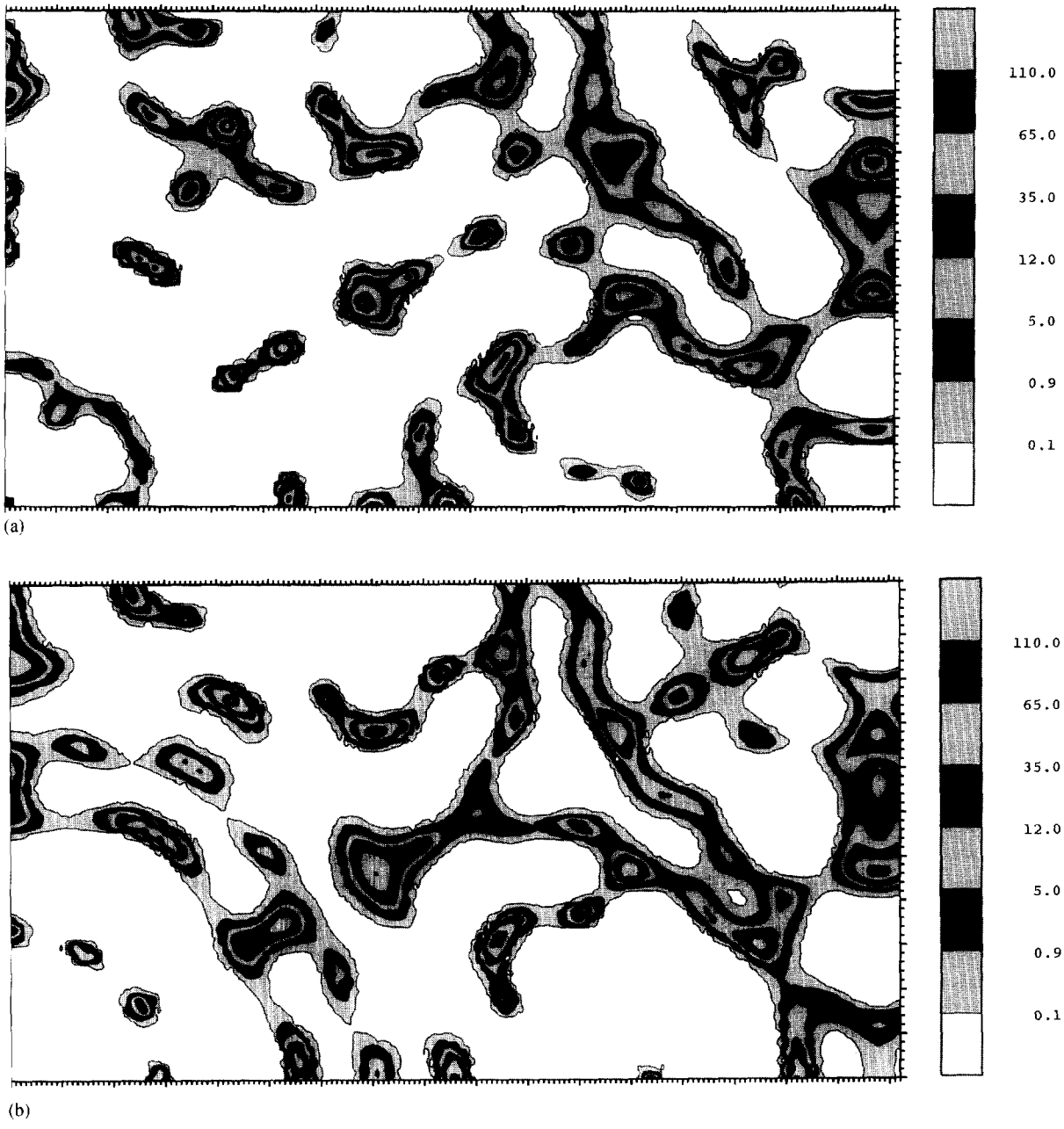

Fig. 6. ME maps calculated from two fluctuations of the X-ray data around their measured values.

density features. Fig. 10 displays the Fourier synthesis of the ED structure factors obtained by Eq. (4). One sees few improvements over the Fourier map obtained from the X-ray data (Fig. 5). The density on the atomic positions is somewhat higher, and the shape of atom 8 is more spherical. On the other hand, there are still many spurious peaks, and some of them are also higher than in the X-ray map, particularly near atom 14, where they are as high as the atom itself. The density is still negative in much of the area of the cell.

Fig. 11 shows the corresponding ME map. The atomic peaks of all atoms are very definite, and higher than in

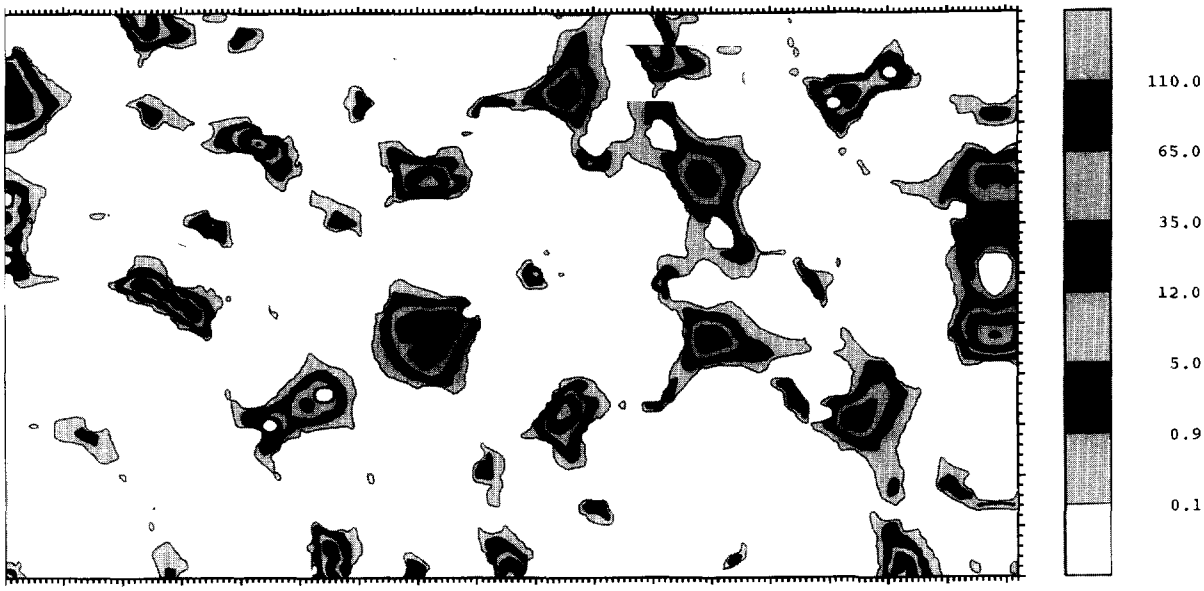

Fig. 7. Lower envelope of X-ray ME maps.

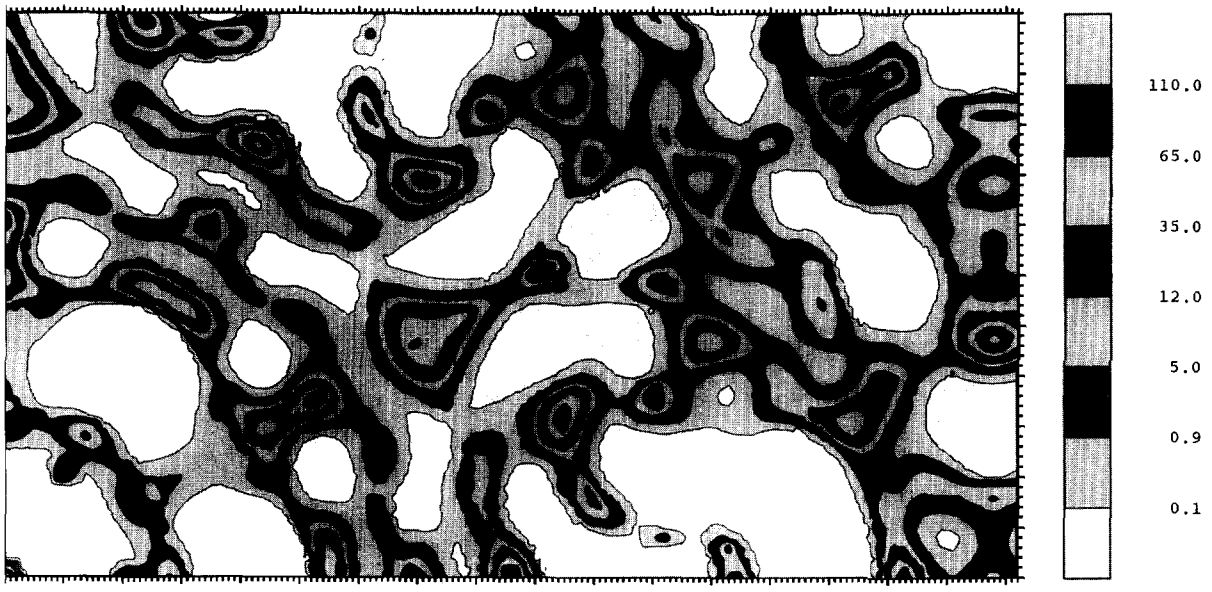

Fig. 8. Upper envelope of X-ray ME maps.

the X-ray map (Fig. 3). The spurious peaks along the diagonal of the figure are still present, but are less significant than in Fig. 3. Some spurious contours, but of low levels, are seen near the origin and between atoms 9 and 10. All atoms have nearly spherical shapes. The highest densities are located at the adatom positions, in accordance with what is expected from the structure. We thus consider this map an improvement over the X-ray one. There is, however, no indication of bondings, and there are significant differences relative to the X-ray map near atoms 4, 12 and 5.

Let us now consider the reliability of the ED ME map. We calculated maps using five fluctuations of the data, one of which is presented in Fig. 12. This map is

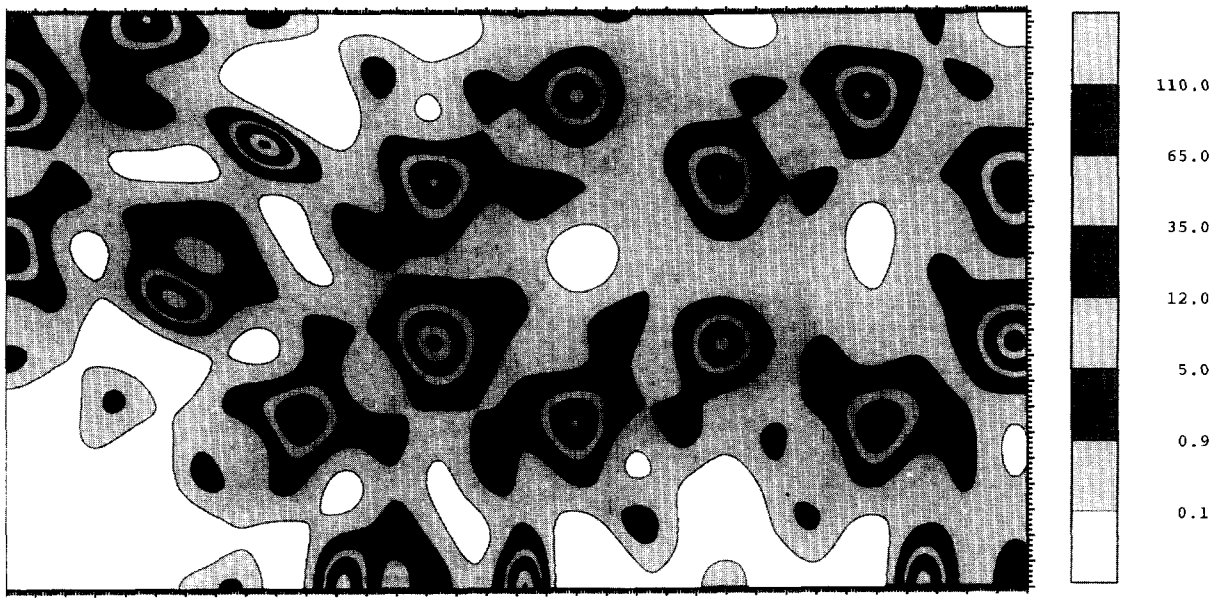

Fig. 9. X-ray ME map from theoretical structure factors calculated using least-squares refined atomic positions.

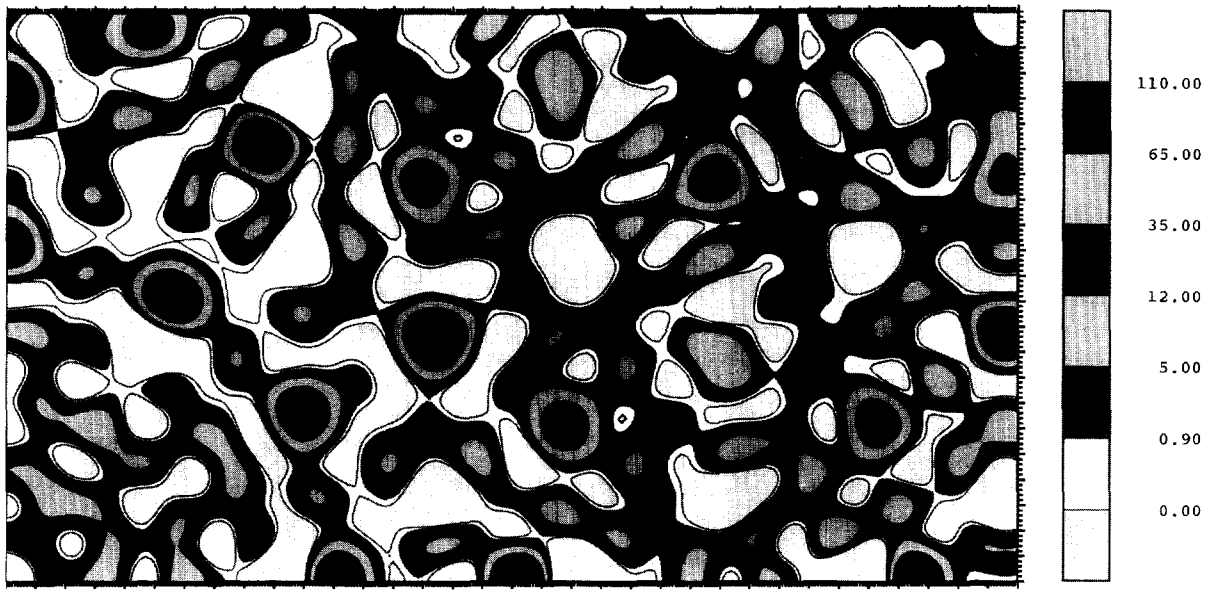

Fig. 10. Fourier synthesis map of structure factors calculated from ED data using Eq. (4).

significantly different from the one obtained from the original data, which is a symptom of little reliability. Figs. 13 and 14 show the upper and lower envelopes resulting from the fluctuations. The lower map merely shows the positions of the atoms; therefore, anything else is uncertain. The fluctuations in the ED maps are bigger than in the X-ray case, even though the map from the original data is more satisfactory. We also observe that convergence is very difficult for the ED fluctuations, but not for the original data themselves. This could be an indication that the uncertainties in the ED data set are overestimated.

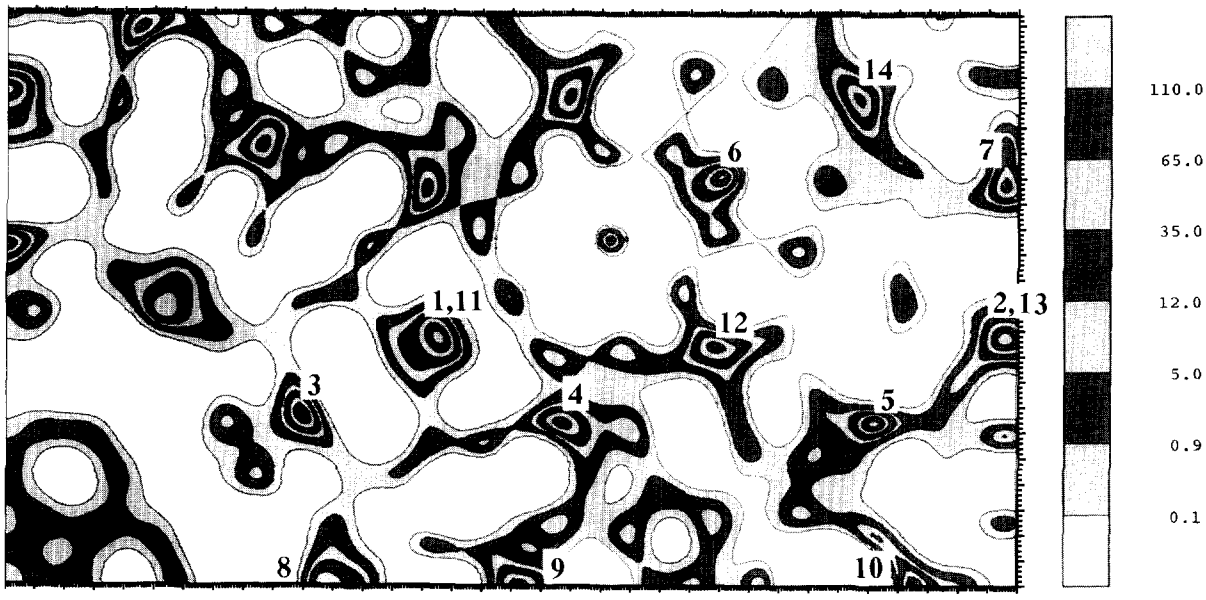

Fig. 11. ME map calculated from ED data using Eq. (4).

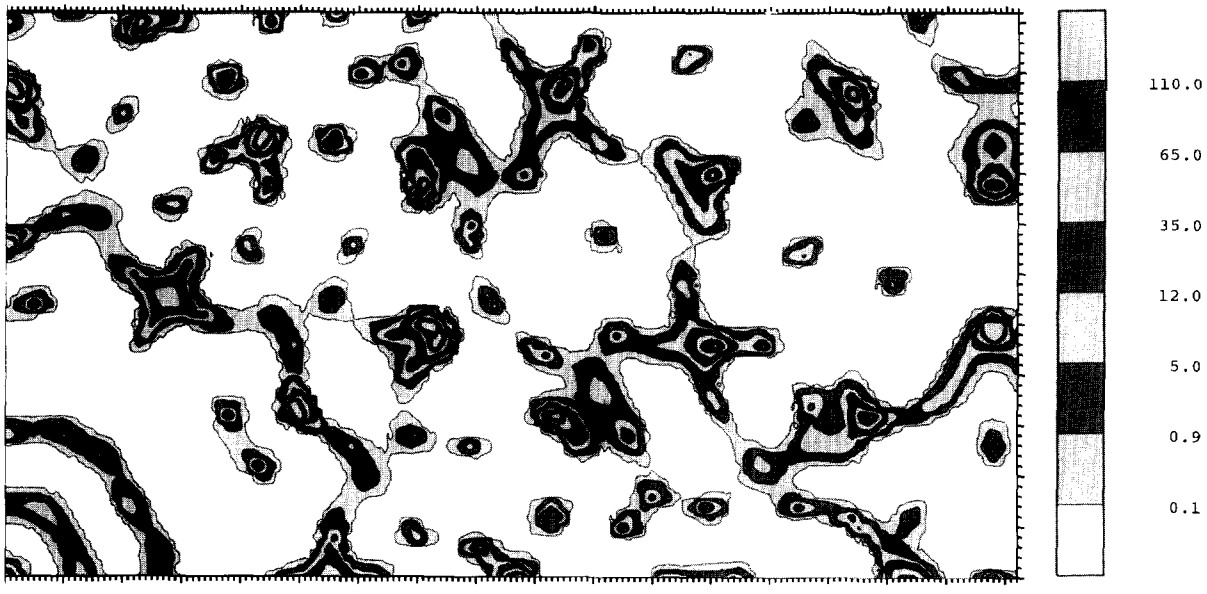

Fig. 12. ME map calculated from a random fluctuation around the structure factors obtained from ED data using Eq. (4).

We observed above that there is a difference in the signs of some reflections produced by the refined coordinates and the DAS ones. The ME map calculated using the signs defined by the DAS coordinates shows differences from the one in Fig. 11 that are within the fluctuations. This means that we do not need to start from refined coordinates. If the data are precise enough it may even be possible to proceed by iterations, recalculating the signs from the measured ME density maxima, then recalculating the ME density, until convergence.

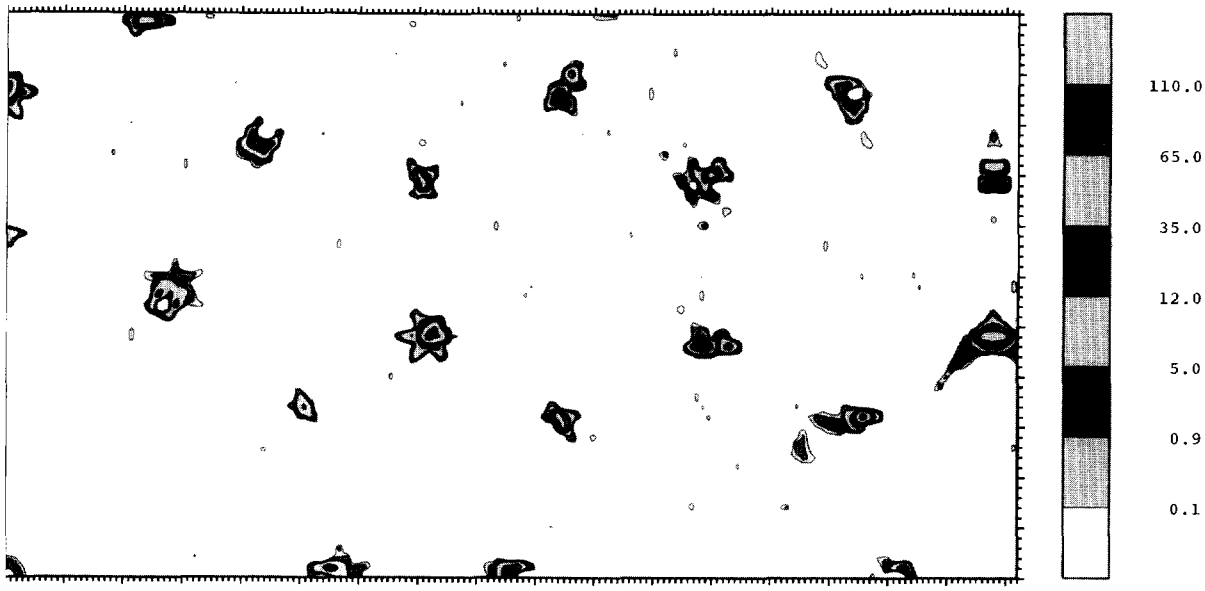

Fig. 13. Lower envelope of ED ME maps.

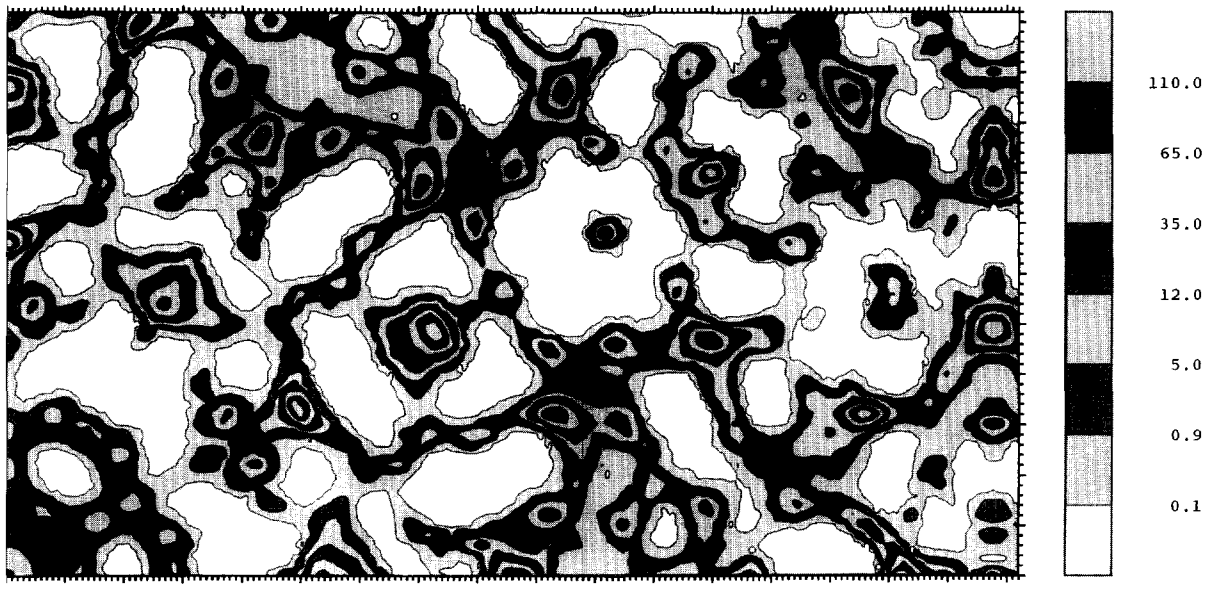

Fig. 14. Upper envelope of ED ME maps.

Fig. 15 shows the ME map calculated using the theoretical ED structure factors for the 193 reflections in our data set. There is an improvement over the corresponding "ideal" X-ray map (Fig. 9) notably in the shapes of atoms 3, 8 and 9. The peak densities are highest for the adatom positions, and are smallest at the stacking-fault atomic positions. There are also some slightly higher ridges between atoms that could be taken for bondings, since they are in the directions predicted by the DAS model, especially between atoms 1-11 and 4, 5, 2-13 and 7. The question then arises of how can bondings be seen from structure factors calculated from spherical atoms.

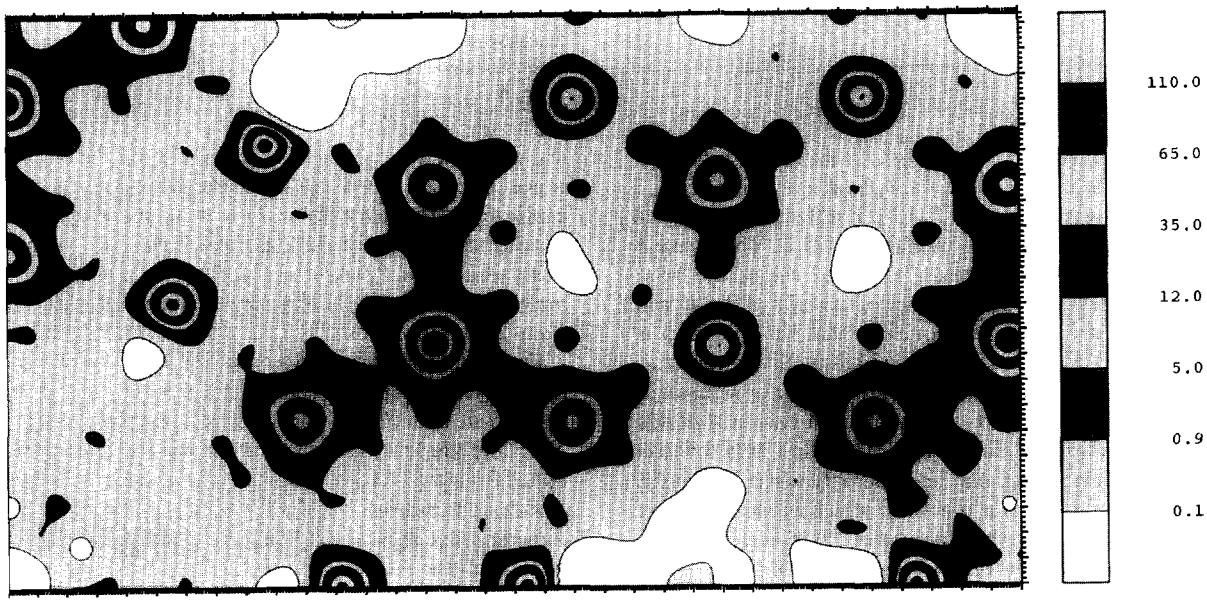

Fig. 15. ME map from theoretical ED structure factors for reflections in the ED data set calculated using X-ray refined atomic positions.

There are two contributions. First, the atomic electron-density tails might superpose between the atoms, increasing the density there. Second, the limited structure-factor set does not faithfully describe the initial spherical atomic density. Thus ME might hint to bondings because it does not assume that forbidden reflections have null intensities. However, even in this case the bonding densities would be incorrect, since the necessary information for their correct evaluation is absent from the structure factors. We also observe that the ME iterations do not reproduce well the lowest-order reflection (2 1 0), when all the 193 reflections of the ED data set are used, such as in Fig. 15, even though $\chi^2 = 2 \times 10^{-4}$. For the smaller X-ray data set this phenomenon does not appear. This might indicate that the more complete ED data set is not self-consistent, in the sense that some contribution is not matched by the structure factor of the (2 1 0) reflection. Removing this reflection from the data set results in improved covergence, but there is no visible effect in the map.

In order to clarify the origin of the "bonding" ridges in Fig. 15, we calculated the theoretical density distribution resulting from a simple superposition of the atomic electron densities of isolated atoms. Since the wave functions are not easily available, we used the atomic scattering factor f for X-rays. The atomic electron density ρ_a is given by

$$\rho_a(r) = 32\pi \int_0^s s^2 f(s) \frac{\sin 4\pi rs}{4\pi rs}\, ds, \tag{5}$$

with $s = \sin\theta/\lambda$. We used the new representation of f as a sum of Gaussians by Waasmaier and Kirfel [16], which is very precise and valid over an extended range. In this representation,

$$f(s) = D + \sum_{j=1}^{5} a_j e^{-b_j s^2}, \quad 0 \leqslant s \leqslant K,$$

where $K = 6\ \text{Å}^{-1}$ and D is a constant. The integral in Eq. (5) can then be evaluated analytically, with the result

$$\rho_a(r) = 32\pi K^3 \frac{\sin 4\pi rK - 4\pi rK \cos 4\pi rK}{(4\pi rK)^3}$$

$$+ \sum_j 8a_j \left\{ \left(\frac{\pi}{b_j}\right)^{3/2} e^{-(2\pi r)^2/b_j} \mathscr{R}[\text{erf}(\sqrt{b_j}K - i2\pi r/\sqrt{b_j})] \right.$$

$$\left. - \frac{\sin 4\pi rK}{2rb_j} e^{-b_j s^2} \right\}, \tag{6}$$

where erf(z) is the error function and $\mathscr{R}$ indicates the real part of a complex number.

Our X-ray and ED data sets contain only reflections with $l = 0$, which implies that the two-dimensional reconstructed density obtained either by Fourier synthesis or ME is the integral of the three-dimensional density over z. Therefore, we must calculate the two-dimensional

atomic density σ given by

$$\sigma(x, y) = \int_{-z}^{z} \rho_a(\sqrt{x^2 + y^2 + z^2})\,dz.$$

σ is a function of $r' = \sqrt{x^2 + y^2}$, and is quite different from $\rho_a(r')$.

The density of the Si(1 1 1) 7×7 surface was obtained by superposition of the atomic density σ. The result is shown in Fig. 16, where "bonding" ridges are seen. Clearly, they are a consequence of the tails of the atomic density distribution. We conclude that the ME map of Fig. 15 is correct, and is in fact a high-quality reconstruction. High-level ridges between atoms are not necessarily evidence of electron re-arrangement in chemical bonds, as is sometimes claimed. The distinction between true and pseudobondings can be done only when the density distribution is known precisely, which is often difficult. We also point out that the correct map of Fig. 16 has higher peaks than those of Figs. 9 and 15.

The fringes seen in the low-density regions of Fig. 16, which are produced by the oscillations of the distribution $\rho_a(r)$ [Eq. (6)], are due to the truncation of the atomic scattering factor to the range $s \leqslant 6\ \text{Å}^{-1}$. They are quite evident, even when such an extended range of s values is used. This is an indication of the importance of truncation effects in Fourier reconstructions. Calculation of the density profile $\rho_a(r)$ by ME would probably produce a better map. However, one could argue that the pseudobondings might be an artifact of ME, since we would be discussing only ME reconstructions, the theoretical one (Fig. 16) and that from ED data (Fig. 15). Calculating ρ_a by Fourier transform avoids this possibility.

The importance of the maps calculated with theoretical structure factors is not their doubtful physical significance. They are important because they show that the problems in the maps obtained from experimental data are due to the data quality and not to the ME method. With accurate and precise data ME reconstruction could provide detailed information on electron densities even from a few reflections.

For a fair comparison between ME and Fourier synthesis it is necessary to consider the Fourier map of the theoretical structure factors, which is presented in Fig. 17. There are few differences compared to the map obtained from the ED data (Fig. 10). The peak heights, both atomic and spurious, are slightly higher in the latter, and some negative regions have become positive. We also see how much the ME map is better than the Fourier synthesis, for these relatively small numbers of reflections.

5. Conclusion

We have calculated the electron-density distribution for the Si(1 1 1) 7×7 surface from X-ray and electron-diffraction data using the maximum-entropy method. The maps clearly show all the 102 atoms of the

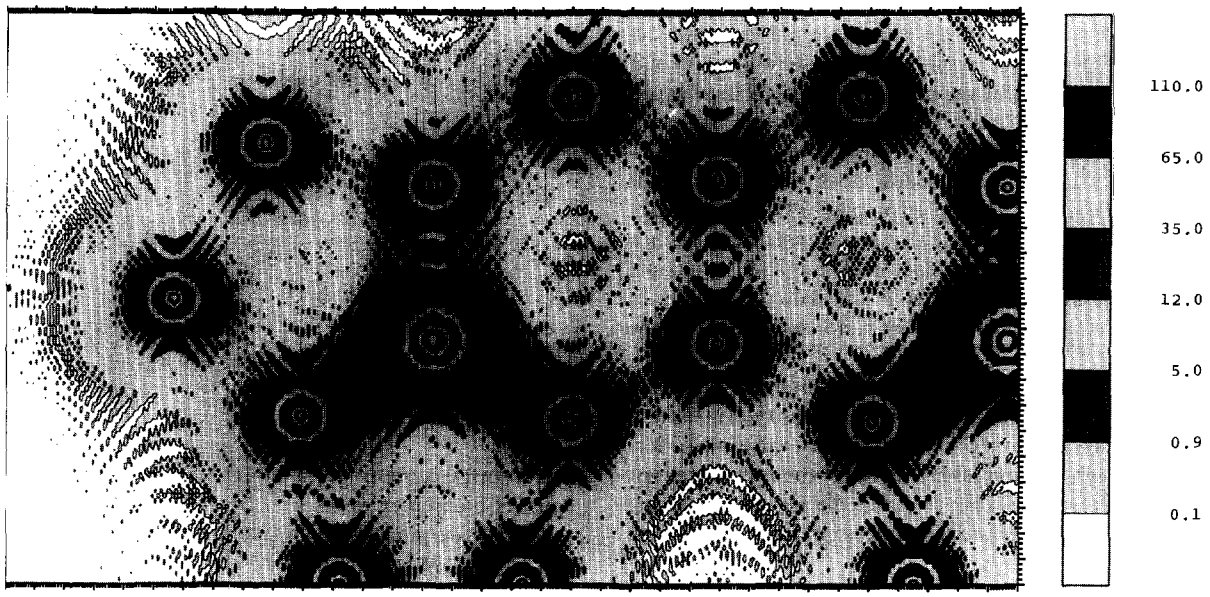

Fig. 16. Density map calculated from the theoretical atomic scattering factor. The atoms in the upper left corner do not appear because they have not been included in the calculation.

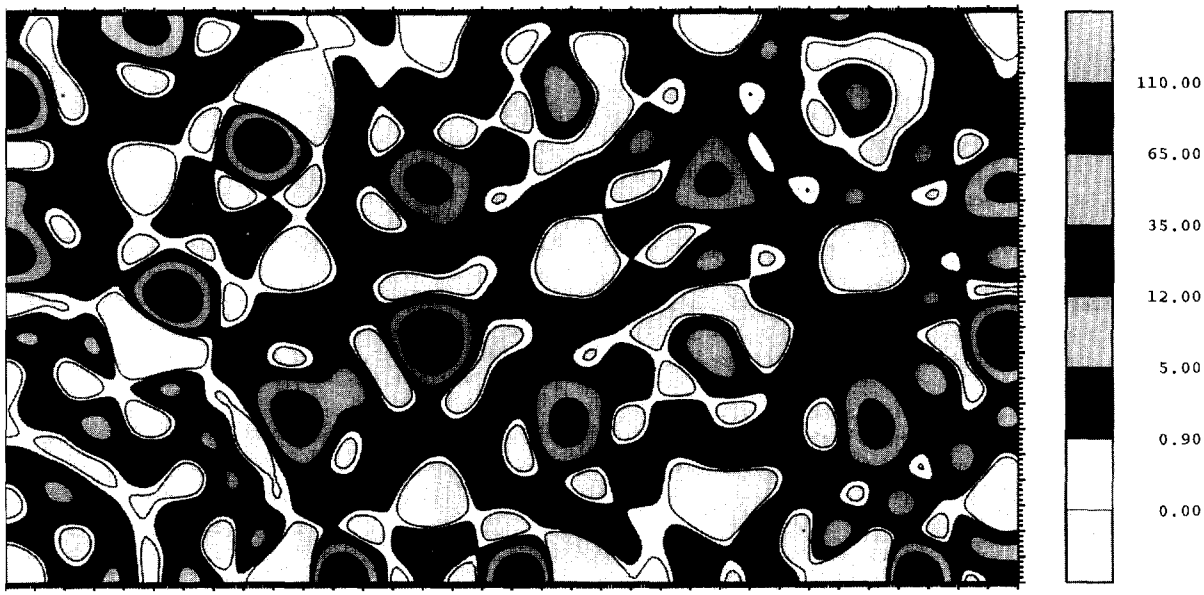

Fig. 17. Fourier synthesis map from the same structure factors as Fig. 15.

Takayanagi dimer-adatom-stacking-fault model. The atomic coordinates are in good agreement with those obtained by a standard crystallographic least-squares fit. The expected electron bondings between atoms are not apparant in the maximum-entropy maps. This is shown to be due to insufficient precision and accuracy of the data.

We also addressed the issue of the reliability of the ME method. It is known that the ME calculation does not produce a satisfactory residue distribution when $\chi^2 = 1$ and this has raised doubts about the correctness of the ME distributions. We have shown that these fears are not justified because the ME calculation is not a parameter-fitting process, so that the statistical significance of the χ^2 is not applicable. Instead, the ME calculation must be carried on until all the data are reproduced very closely. The uncertainty in the resultant distribution is directly related to the data errors, and we have proposed a method to identify the features of the distributions that can be trusted.

One may inquire whether ME produces correct distributions from incomplete information. It has been shown [17] that ME is one member of a family of reconstruction methods that produce sharp peaks and flat baselines. While this is true, however, it has also been shown [18] from fundamental principles that ME is the only method to obtain a probability distribution from the available information without introducing any bias or implicit hypothesis. This makes ME a special technique. It does not mean that it will correctly overcome the limitations of the available information and produce the correct solution, but it means that ME is the only unbiased method to obtain the solution.

To judge whether the solution is correct in the case of the Si(1 1 1) 7×7 surface, we calculated density maps from error-free theoretical structure factors. The result is very good, and this qualifies the ME method as a promising tool to obtain detailed information on surface structures. Even if only a few structure factors are available, ME will produce reliable, unbiased detailed density maps, if the data are precise and accurate. On the other hand, it is clear that if the data do not contain the information to reliably determine the details of the density distribution, ME, by its very nature, will be the last method to produce these details. Modest structure information is obtained on the Si(1 1 1) 7×7 surface in the present work, which applied the ME method, for the first time, to two-dimensional surface structures. Nevertheless, this technique is quite promising for accurate determination of surface structures from diffraction data.

Acknowledgements

We thank Ray Twesten for providing us the ED data and pointing out the misprint in the published coordinates. We also thank A. Preusser for assistance in the customization and use of the contour plot program.

References

[1] I.K. Robinson, in: Handbook on Synchrotron Radiation, Vol. 3, eds. G. Brown and D.E. Moncton (North-Holland, Amsterdam, 1991) p. 221.
[2] D.M. Collins, Nature 298 (1982) 49.
[3] K. Takayanagi, Y. Tanishiro, S. Takahashi and M. Takahashi, Surf. Sci. 164 (1985) 367.
[4] I.K. Robinson, W.K. Waskiewicz, P.H. Fuoss and L.J. Norton, Phys. Rev. B 37 (1988) 4325.
[5] A.C. Wilson (ed.), International Tables for Crystallography, Vol. C, The International Union of Crystallography, 1992, p. 478.
[6] R.D. Twesten and J.M. Gibson, Ultramicroscopy 53 (1994) 223.
[7] C.A.M. Carvalho and H. Hashizume, Report of RLEM-TIT, No. 17, Tokyo Institute of Technology (1992) p. 47.
[8] N. Sudo, H. Hashizume and C.A.M. Carvalho, Powder Diffraction 10 (1995) 34.
[9] H. Hiraguchi, H. Hashizume, O. Fukunaga, A. Takenaka and M. Sakata, J. Appl. Crystallogr. 24 (1992) 286.
[10] W. Jauch and A. Palmer, Acta Crystallogr. A 49 (1993) 590.
[11] W. Jauch, Acta Crystallogr. A 50 (1994) 650.
[12] G. Binnig, H. Rohrer, Ch. Gerber and E. Wibel, Phys. Rev. Lett. 50 (1983) 120.
[13] R.M. Tromp, R.J. Hamers and J.E. Demuth, Phys. Rev. B 34 (1986) 1388.
[14] R.J. Hammers, R.M. Tromp and J.E. Demuth, Phys. Rev. Lett. 56 (1986) 1972.
[15] A. Preusser, ACM Trans. Math. Software 15 (1989) 79.
[16] D. Waasmaier and A. Kirfel, Acta Crystallogr. A 51 (1995) 416.
[17] R. Nityananda and R. Narayan, J. Astrophys. Astron. 3 (1982) 419.
[18] J.E. Shore and R.W. Johnson, IEEE Trans. Inform. Theory 26 (1980) 26.